Electrochemical Measurements of the Lateral Diffusion of Electroactive Amphiphiles in Supported Phospholipid Monolayers

Elisabeth Torchut, Jean-Marc Laval, Christian Bourdillon, and Marcin Majda

Laboratoire de Technologie Enzymatique, URA 1442 du CNRS, Université de Compiègne, BP 649, 60206 Compiègne, France; and Department of Chemistry, University of California at Berkeley, Berkeley, California 94720 USA

ABSTRACT Chronocoulometry was used to characterize the fluidity and lateral diffusion coefficient of supported phospholipid bilayer assemblies. The bilayers were formed on the inner surfaces of the microporous template films of aluminum oxide on gold electrodes. The lipid monolayers were formed by adsorption and fusion of phospholipid vesicles on alkylated oxide surfaces. Octadecyltrichlorosilane (OTS) was used in the initial alkylation step. The surface concentration of the lipids in monolayer assemblies was measured by a radioactive assay method. Surface densities corresponding to 48 ± 10 Å^2/molecule (DPPC) and 56 ± 11 Å^2/molecule (DMPC) were obtained (for exposure times >120 min) largely independent of the temperature of the vesicle's fusion (below or above chain-melting transition). Octadecylviologen ($C_{18}MV^{2+}$) was used as an electroactive probe species. Its limiting lateral diffusion coefficient in DMPC monolayers was 5×10^{-8} cm^2/s, measured as $C_{18}MV^{2+}$ mole fraction extrapolated to 0 decreasing linearly from 20 to below 1 mol %. Linear Arrhenius plots for $C_{18}MV^{2+}$ diffusion in DMPC monolayers were obtained with slopes of ~40 kJ/mol between 18 and 45°C, demonstrating homogeneity and fluidity of the lipid monolayers. Chronocoulometry was also used to obtain lateral diffusion coefficient of ubiquinone in DMPC/OTS bilayers. A value of 1.9×10^{-8} cm^2/s at 30°C was obtained.

INTRODUCTION

Lateral diffusion of amphiphilic and hydrophobic electron carriers in the plane of phospholipid membranes is one of the key elements involved in the transport processes associated with photosynthesis and other membrane processes (Hackenbrock, 1981). Various models of biological membrane systems have been used to study the dynamics of long-range transport phenomena (Gennis, 1989). Among them, phospholipid layers which are supported on solid substrates have been increasingly popular in recent years. In this context, three techniques of membrane formation and/or reconstitution should be mentioned: 1) "horizontal touch" method, in which a lipid monolayer initially spread and compressed on the air-water interface is transferred onto an alkylated solid support simply by bringing the support surface in contact with the surface monolayer (Tscharner and McConnell, 1981; McConnell et al., 1986); 2) mono- or bilayers of phospholipids transferred by the Langmuir-Blodgett deposition method (Tamm and McConnell, 1985; McConnell et al., 1986); 3) small unilamellar vesicles spontaneously fused onto hydrophilic or alkylated surfaces to form planar membranes when solid substrate is incubated in a vesicles solution (Brian and McConnell, 1984; Singh and Keller, 1991; Kalb et al., 1992). The latter technique is especially valuable when a goal of an experiment is to reconstitute an entire membrane with all its naturally occurring components.

The artificial lipid membranes obtained by any of these techniques have proven to be very useful in the studies of lateral diffusion of phospholipids, membrane proteins, and other membrane components. In such studies, fluorescence recovery after photobleaching (FRAP) has been a technique most frequently used (Tscharner and McConnell, 1981; Cherry, 1979; Peters and Beck, 1983; Kim and Yu, 1992; Tamada et al., 1993). This technique covers a substantial range of diffusion rates extending from about 10^{-6} cm^2 s^{-1} to 10^{-10} cm^2 s^{-1}. However, it requires fluorescence labeling of a fraction of the diffusing molecules. This can be a real constraint when diffusion of low molecular weight and minor membrane components such as ubiquinone are studied since the relative change in the molecular weight and the conformational changes induced by grafting fluorescent labels can be substantial and can affect both the location and the lateral mobility of the molecule in question.

Recently, application of the electrochemical methods in the determination of the diffusion coefficient of the electroactive molecules has been extended to amphiphilic monolayer (Charych et al., 1991; Majda, 1993) and bilayer assemblies (Miller et al., 1988; Goss et al., 1988; Majda, 1991; Goss and Majda, 1991; Lindholm-Sethson et al., 1993). These methods are particularly advantageous in the studies of the lateral mobility of natural and artificially introduced electron transfer mediators and carriers, since the intrinsic electrochemical activity of those species circumvents the need for labeling. Electrochemical methods are very well suited for the investigations of the dynamics of transport processes, since faradaic current is directly proportional to the flux, $D \, \partial C/\partial x$ or the arrival rate of the electrochemically active molecules at the electrode surface (Bard and Faulkner, 1980a)

$$i = n \, FAD(\partial C/\partial x)_{x=0} \qquad (1)$$

where n is the number of electrons involved in an elementary reaction, F is Faraday constant, and D and C = C(x, t) are the diffusion coefficient and the concentration of the electroactive species. In the potential step techniques such as chronocoulometry (Bard and Faulkner, 1980b) discussed below, application of a square potential pulse generates, after charging of the solution/electrolyte interface, an instantaneous concentration gradient and simultaneously initiates current flow. The analysis of the integral of current evolution with time gives the value of D. Thus this approach is analogous to the FRAP technique.

From an experimental point of view, the major challenge in implementing electrochemical methods involves the design of microelectrodes that can be positioned perpendicular to the monolayer assembly. One such design involves electrodes coated with microporous aluminum oxide films (Majda, 1991; Miller and Majda, 1986). Amphiphilic bilayer assemblies can then be formed on the inner surfaces of the oxide template. The unique geometry of the template produces an array of cylindrical bilayers which are oriented perpendicularly to the electrode surface (see Fig. 1).

The goal of this study was to use the microporous oxide film technique in the direct electrochemical investigations of the lateral diffusion of redox-active molecules in supported bilayers involving dimiristoyl and dipalmitoyl phosphatidyl-

cholines. We demonstrated that a phospholipid containing bilayer can be formed on the inner surfaces of aluminum oxide films. We relied in this step on fusion of lipid vesicles with the oxide surfaces that were previously alkylated by self-assembly of octadecyltrichlorosilane (OTS). We then described the electrochemical behavior and the lateral diffusion of an electroactive amphiphilic probe species, N-methyl-N'-octadecyl-4,4'-bipyridinium chloride (octadecylviologen, $C_{18}MV^{2+}$) as a function of its concentration in lipid monolayers. In the limit of low $C_{18}MV^{2+}$ surface concentrations, these measurements yield the fluidity of the lipid monolayers. Finally, we report preliminary data concerning the lateral diffusion of ubiquinone 50, a naturally occurring electron carrier, incorporated in the hydrocarbon region of our bilayer assemblies.

MATERIALS AND METHODS

Reagents

L-α-Dimyristoyl phosphatidylcholine (DMPC), L-α-dipalmitoyl phosphatidylcholine (DPPC), and ubiquinone 50 (Q_{50}) were purchased from Sigma Chemical Co. (St. Quentin Fallavier, France, synthetics >99% pure). L-α-1,2-Di(1-^{14}C)palmitoyl phosphatidylcholine (^{14}C-DPPC) was from Amersham (Les Ulis, France, 50 mCi/mmol). N-methyl-N'-octadecyl-4,4'-bipyridinium dichloride ($C_{18}MV^{2+}$) was synthesized according to Pileni et al. (1980). Octadecyltrichlorosilane (OTS) (Aldrich, Strasbourg, France) was vacuum-distilled before use. Hexadecane (Aldrich) was dried with a desiccated molecular sieves. All other chemicals were reagent grade.

Preparation of the aluminum oxide-coated gold electrodes

The basic procedure was similar to that described previously by Miller and Majda (1986) and modified by Parpaleix et al. (1992). Briefly, aluminum oxide films were produced by anodization of 1-mm-thick aluminum foil (Al 99.95%, Merck, Darmstadt, Germany) at 65 V for 50 min in a 0.37 M H_3PO_4 solution thermostated at 25 ± 0.5°C. Anodization under these conditions produces uniformly porous aluminum oxide films ~3 μm in thickness with internal surfaces areas of 45 cm^2 (±15%) per cm^2 of the geometric oxide film area (Miller et al., 1988). Anodic films were separated from the aluminum substrate by immersion of the anodized foil in a saturated aqueous $HgCl_2$ solution. The removal of the barrier layer from free-standing oxide films, a critical step in the fabrication procedure, was carried out by floating ~1 cm^2 sections of Al_2O_3 films on a NaOH solution as described previously (Parpaleix et al., 1992). The average thickness of these films was 3.0 ± 0.3 μm based on scanning electron microscopy of the cross-sections of 10 different oxide samples from three different batches.

Fabrication of the gold electrodes coated with OTS-treated oxide films involved the following additional three steps. Dried oxide films were transferred into a freshly prepared 2% (v/v) OTS solution in hexadecane. After a 15-min OTS self-assembly, they were rinsed extensively with toluene and transferred into a vacuum deposition apparatus (Edwards model E306A), where they were coated with ~2-μm-thick gold films. Finally, gold-coated oxide films were mounted on the tip of glass tubing (3 mm in diameter) according to a procedure as described (Miller and Majda, 1986). The geometrical surface area of the porous aluminum oxide-coated gold electrodes was 0.071 cm^2. The internal surface area of an oxide film of an individual electrode was ~3.2 cm^2. This value is burdened with ±15% error due to uncertainties in the determination of the film thickness and in the extent to which its internal structure is modified during the removal of the barrier layer.
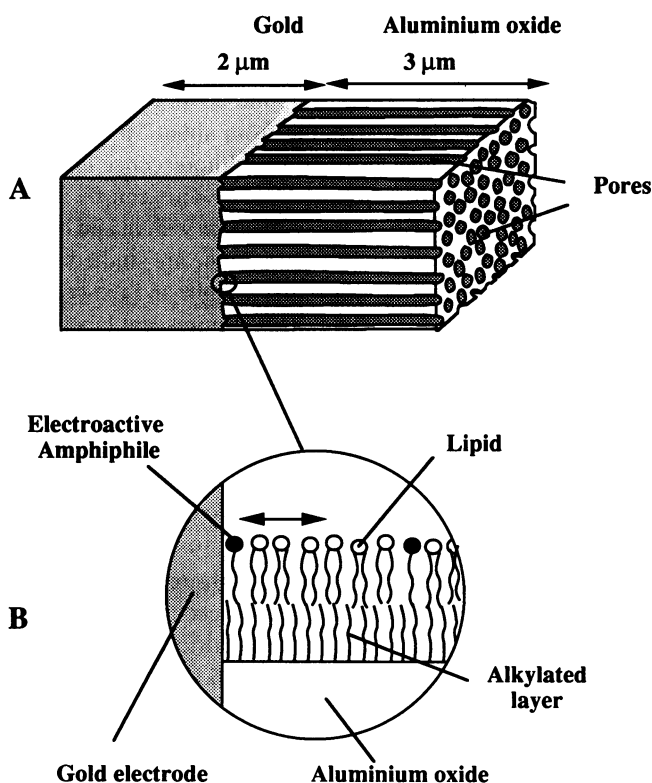

FIGURE 1   (A) Structure of a porous aluminum oxide film attached to a gold electrode. The average pore diameter of the films was 90 ± 10 nm. For more details see Miller et al. (1988) and Parpaleix et al. (1992). (B) Schematic structure of a OTS/phospholipid bilayer assembled on the inner surfaces of the porous aluminum oxide film in contact with the electrode surface.

Electrochemical measurements

An anaerobic electrochemical cell was fitted with three electrodes: a working microporous aluminum oxide film electrode, a saturated calomel reference electrode (E_{SCE} = 0.245 V vs. normal hydrogen electrode at 25°C), and a platinum foil auxiliary electrode. The latter was contained in a compartment separated from the main compartment by a glass frit. Gentle bubbling of argon was used to deaerate solutions and to blanket the main compartment of the cell. Temperature (15–45°C) was controlled by water circulation in the outer jacket of the cell.

A PAR model 273 potentiostat controlled by a PC computer and model 270 software package (EG & G Princeton Applied Research, Princeton, NJ) was used in cyclic voltammetric and chronocoulometric experiments. The voltammetric curves were recorded on an XY recorder (model BD90, Kipp and Zonen, Delft, Holland). All electrochemical measurements were done in 0.1 M phosphate buffer solutions, pH 7.0.

Formation of supported monolayer assemblies

Direct fusion of unilamellar vesicles of lipids on the inner surfaces of OTS-treated microporous aluminum oxide templates followed the procedure previously described by Brian and McConnell (1984). About 3 mg of a lipid was resuspended from the walls of a glass tube by vigorous vortexing in 5 ml of 0.1 M phosphate buffer, pH 7. This solution was sonicated to clarity four times for 3 min with a Branson B12 sonicator set at 40 W power (Danbury, CT). Despite an ice bath and 5-min rest intervals between each sonication, the final temperature reached about 40°C. This prepared stock solution (7.0 10⁻⁴ M) was used to prepare more dilute solutions in the course of the following week. The microporous oxide film electrodes were first wetted with methanol and then rinsed with 0.1 M phosphate buffer in three different baths. A wetted electrode was then transferred and incubated in a vesicle solution at 30°C. Before use, the electrodes were rinsed with 0.1 M phosphate buffer for at least 10 min.

Self-assembly of $C_{18}MV^{2+}$ on the OTS-treated surfaces is straightforward due to relatively high solubility of this compound (critical micelle concentration for $C_{18}MV^{2+} \cdot 2Cl^-$ was reported to be 0.82 mM by Krieg et al., 1981). $C_{18}MV^{2+}$ self-assembly was done by incubating the OTS-treated oxide electrodes in 5.0 × 10⁻⁴ M $C_{18}MV^{2+}$ solution in the 0.1 M phosphate buffer for 30 min followed by rinsing with distilled water. Supported lipid monolayers containing ubiquinone were prepared as follows. Samples of a lipid and ubiquinone were solubilized together in chloroform. A sample of the chloroform solution was dried in a glass tube by a stream of nitrogen and then incubated in vacuum for 1 h. Vesicles and supported monolayers were then prepared as described above.

Radioactive measurements

Radioactively labeled lipid, ¹⁴C-DPPC, was introduced at a 1 mol % level into the lipid solutions in chloroform. Subsequently, the same procedures described above were followed to prepare supported monolayer assemblies in the microporous oxide films on gold electrodes. In the final stage of vesicles adsorption and fusion, a small piece of paraffin tape was rolled round the tip of a glass tube electrode body to prevent the direct adsorption of lipids on the glass surrounding the oxide layer. The piece of paraffin tape was then carefully removed before the subsequent rinsing steps. Ten-milliliter aliquots of a buffer solution, maintained at the same temperature as the vesicle solution, were used in three rinses of 10 min each. The last rinsing buffer solution contained negligible quantity of the radioactive lipid. Lipids (both "cold" and radioactively labeled) forming supported bilayer assemblies in the oxide films at electrodes could be easily extracted from the oxide layer by a 5-min incubation of an electrode in 2 ml of methanol. This extraction procedure was very effective, since the second 5-ml aliquot of methanol exhibited only negligible radioactivity following the second incubation of the electrode. The measurements of radioactivity of the methanol samples were carried out following an addition of 15 ml of a liquid scintillation cocktail with a model LS8000 scintillation counter (Beckman, Fullerton, CA). Signal integration was carried out for 10 min with the samples exhibiting typically about 1500 cpm.

RESULTS AND DISCUSSION

Formation of supported phospholipid and $C_{18}MV^{2+}$ monolayers

It is now well established that exposure of an alkylated surface, such as those obtained by self-assembly of OTS on glass or aluminum oxide, to aqueous solutions of an amphiphile or a suspension of unilamellar vesicles leads to a spontaneous assembly of an ordered monolayer with the tail-to-tail conformation characteristic for lipid bilayers (Brian and McConnell, 1984; Kalb et al., 1992; Miller et al., 1988). The bilayer formation on planar surfaces can be monitored and investigated by infrared (Maoz and Sagiv, 1983) or fluorescence spectroscopy (in the latter case, the presence of a low concentration of labeled lipids is necessary; see, for example, Brian and McConnell, 1984).

Electrochemical detection can be used if the monolayer contains an electrochemically active amphiphile. In this study, we used octadecylviologen ($C_{18}MV^{2+}$). In such cases, a coulometric assay can be carried out to determine the surface concentration of the electroactive species. Considering our primary experimental goal of circumventing the need for lipid labeling with a redox probe, we developed two approaches to study the formation process of the supported lipid bilayers in the porous aluminum oxide films. The first approach relies on inhibition of $C_{18}MV^{2+}$ self-assembly by adsorption and fusion of lipid vesicles carried out as an initial step of the assembly procedure. In this approach the extent of $C_{18}MV^{2+}$ assembly is determined electrochemically. In the second approach, we use direct measurements of the level of radioactivity in the self-assembled ¹⁴C-labeled lipid.

We first describe voltammetric characterization of $C_{18}MV^{2+}$ self-assembly in OTS-treated porous aluminum oxide films. Self-assembly was carried out by a 30-min exposure of a treated electrode substrate to a 5 × 10⁻⁴ M $C_{18}MV^{2+}$ solution in 0.1 M phosphate buffer. Fig. 2A shows a cyclic voltammogram recorded at one such electrode after it was rinsed, following the assembly step, and then transferred to a pure buffer solution. The symmetrical bell shape of the current peaks is a characteristic signature of a system in which electroactive material is confined to a thin film near the electrode surface (Bard and Faulkner, 1980c). In such cases, the entire population of the redox species can diffuse rapidly to the electrode surface to be reduced and then reoxidized on the time scale of a single voltammetric scan. As a result, the cathodic and anodic currents decay to the background level at the end of each segment of the voltammetric cycle.

In the present case, the reversible processes occurring at the gold electrode involve a one-electron redox reaction:
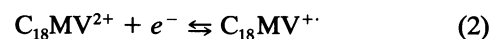
$$C_{18}MV^{2+} + e^- \leftrightarrows C_{18}MV^{+\cdot} \qquad (2)$$

Since $C_{18}MV^{2+}$ is confined to only a 3-μm-thick film of aluminum oxide, all octadecylviologen molecules can access the electrode surface during a 50 mV/s scan showed in Fig. 2 via lateral diffusion along the OTS/$C_{18}MV^{2+}$ bilayer assembly. Thus, integration of either of the voltammetric peaks
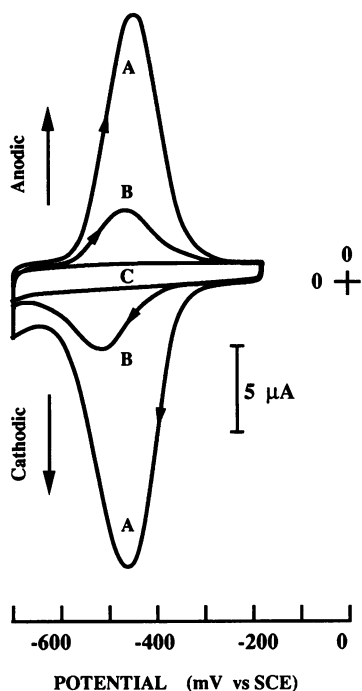
FIGURE 2   Cyclic voltammograms of $C_{18}MV^{2+}$ in OTS-treated porous aluminum oxide films on gold electrodes recorded in 0.1 M pH 7.0 phosphate buffer at 50 mV/s. (A) After a 30-min exposure to a 5.0 × 10⁻⁴ M $C_{18}MV^{2+}$ loading solution and a medium transfer to pure phosphate buffer. (B) Partial inhibition (82%) of $C_{18}MV^{2+}$ assembly observed when an oxide coated electrode was first exposed to 7.0 × 10⁻⁴ M DPPC vesicle solution for 30 min and then treated as in A. (C) Background current recorded after DPPC assembly step only.

gives us the total charge, Q_f, and allows us to calculate the surface concentration of $C_{18}MV^{2+}$. The values of charge and of the stable coverage were found to be ~40 μQ and 140 ± 28 pmol/cm², respectively. Higher surface concentrations can be obtained (by increasing $C_{18}MV^{2+}$ concentration in the self-assembly solution) but are not stable after electrode transfer to a pure phosphate buffer electrolyte where a rapid decrease of the voltammetric signal is observed in the first few scans until it is reduced to the level given above. The stability of OTS/$C_{18}MV^{2+}$ bilayers was discussed previously in detail (Miller et al., 1988). Since the self-assembly is carried out in solutions where $C_{18}MV^{2+}$ concentration is below its critical micelle concentration, we believe that the main driving force of self-assembly and the stability of the resulting bilayers derive primarily from the reduction of the surface free energy of the OTS/water interface. Thus, stability of the $C_{18}MV^{2+}$ monolayers cannot match that of lipid monolayers, as we see below. The voltammetric assay described here was routinely used to screen against oxide-coated electrodes that exhibited $C_{18}MV^{2+}$ loading level below ~35 μQ (corresponding to 120 pmol/cm²).

When an OTS-treated microporous oxide electrode is first exposed to a solution of phospholipid vesicles (see Materials and Methods) and only afterward to a 0.5-mM $C_{18}MV^{2+}$ loading solution, a significantly smaller voltammetric signal

is obtained after the electrode is transferred to a pure phosphate buffer electrolyte (see Fig. 2 B). It is clear that the initial assembly of the phospholipid molecules inhibits self-assembly of $C_{18}MV^{2+}$. We took advantage of this effect in an attempt to quantify the extent of lipid adsorption as a function of the electrode incubation time in a vesicle solution. Our experimental procedure involved first a variable time exposure of a microporous oxide electrode to 7 × 10⁻⁴ M DMPC or DPPC vesicle solution in phosphate buffer at 30°C. After rinsing, the electrodes were transferred to the standard 5 × 10⁻⁴ M $C_{18}MV^{2+}$ solution also thermostated at 30°C for 30 min. Finally, the voltammetric assay was carried out in the pure phosphate buffer electrolyte. To bring an electrode back to its initial conditions before the next experiment, it was rinsed with methanol and then phosphate buffer. The results of this series of experiments are shown in Fig. 3. It is readily apparent that $C_{18}MV^{2+}$ cannot displace phospholipids once they are assembled on the OTS-coated surfaces of the oxide film. Self-assembly of $C_{18}MV^{2+}$ seems to progress to the limit of the available surface area. It is also apparent that this approach gives us an indirect measurement of the kinetics of phospholipid vesicles adsorption and fusion. The rate of adsorption and fusion of DMPC and DPPC vesicles that can be inferred from the data in Fig. 3 is similar to that described recently for adsorption and fusion of 1-palmitoyl-2-oleoyl-phosphatidylcholine vesicles on a Langmuir-Blodgett monolayer of the same lipid transferred vertically on a quartz slide (Kalb et al., 1992). In the sequential lipid-$C_{18}MV^{2+}$ assembly experiments the system was thermostated at 30°C. This temperature is above the chain-melting transition for DMPC (T_m = 24°C) and below that for DPPC (T_m = 41°C) (McConnell et al., 1984). Nevertheless, the data in Fig. 3 exhibit only slightly higher coverage of DPPC.

The effect of the temperature on the surface concentration of the two lipids in the supported bilayer assemblies was investigated in more detail using the radioactive labeling approach. The use of microporous aluminum oxide as a
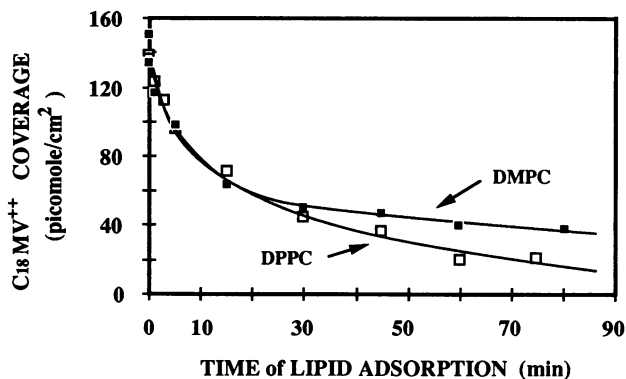

FIGURE 3   Dependence of the surface coverage of $C_{18}MV^{2+}$ in OTS-treated porous aluminum oxide films on the time of exposure of the electrode substrates to 7.0 × 10⁻⁴ M DPPC or DMPC vesicle solutions at 30°C. Self-assembly of $C_{18}MV^{2+}$ followed lipid assembly as in Fig. 2 B.

template for lipid adsorption and fusion proved to be very convenient in these experiments, as the high surface-to-volume ratio of these films assured high signal-to-noise level, even when a low mole fraction of ^{14}C lipid (1 mol %) was used. The adsorption experiments were carried out below and above the transition temperatures for the two lipids. The results in Fig. 4 indicate again that the value of the phase transition temperature of these phospholipids plays little role in affecting kinetics of adsorption and the extent of surface coverage. Similar to the results of Kalb and co-workers (1992), we found that kinetics of the bilayer formation is influenced by the concentration of the lipids in their vesicle solutions, but the latter has no effect on the final surface coverage (the plateau region in Fig. 4). The maximum coverages, obtained after extensive rinsing, were 350 ± 60 pmol/cm^2 for DPPC and 300 ± 50 pmol/cm^2 for DMPC. The relatively high standard deviations reflect primarily the uncertainty of the internal surface area of the aluminum oxide films rather than errors in the measurements of radioactivity.

These values of the stable surface coverage provide a clear indication that both lipids form spontaneously organized monolayer assemblies on the OTS-treated Al$_2$O$_3$ surfaces. The coverages listed above give molecular areas of 48 ± 10 Å^2/molecule for DPPC and 56 ± 11 Å^2/molecule for DMPC. These values correspond to the concentrations in the solid/liquid coexistence region of phospholipid bilayers (Tamm and McConnell, 1985). However, the data in Fig. 4 and additional results presented in the next section suggest strongly that the lipid monolayers in the supported OTS/lipid bilayer assemblies are homogeneous. We discuss this point in more detail in the next section in the context of the lateral diffusion measurements reported there.

We investigated also the stability of the supported lipid bilayers by monitoring the level of radioactivity over long periods of time. Negligible loss of lipid was observed after one day of incubation of a sample in the buffer electrolyte solution at room temperature.
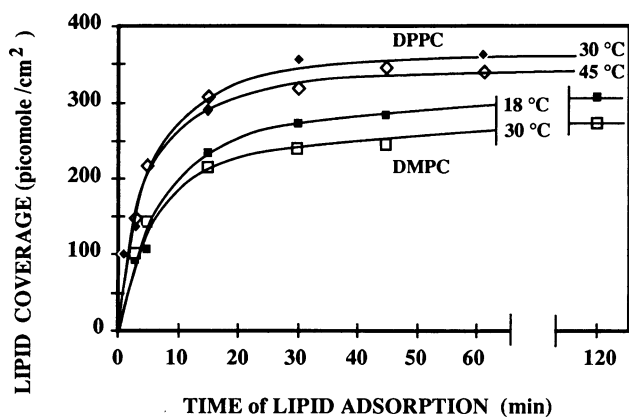

FIGURE 4 Adsorption isotherms of DPPC and DMPC in OTS-treated porous aluminum oxide films obtained by a radioactive assay. Lipids were assembled by exposing oxide coated electrodes to 7.0 × 10^{-4} M lipid vesicle solutions containing 7.0 × 10^{-6} M ^{14}C DPPC.

Measurements of the lateral diffusion coefficients by chronocoulometry

We begin with a description of the electrochemical experiments concerning supported OTS/C$_{18}$MV^{2+} bilayers as a model system. Potential step chronocoulometry is a standard electrochemical technique allowing determination of the diffusion coefficients of electroactive species in solution (Bard and Faulkner, 1980b). This method was extended to the studies of lateral mobilities of the electroactive amphiphiles in bilayer assemblies (Miller et al., 1988; Goss et al., 1988; Majda, 1991; Goss and Majda, 1991; Lindholm-Sethson et al., 1993). In view of the time scale of these types of experiments (0.01–1.0 s), chronocoulometry, similar to the FRAP method, provides a measure of a "long-range" diffusion extending over micrometer distances (Vaz and Almeda, 1991).

In the present case, a typical experiment begins with an initial equilibration of a gold electrode carrying a porous aluminum oxide film with OTS/C$_{18}$MV^{2+} bilayer assemblies (see Figs. 1 and 2 A above) at −0.25 V vs. SCE where no current flows (Miller et al., 1988). Subsequently, a sufficiently large rectangular potential pulse (0.40 V for ∼10 s) is applied to the electrode surface to initiate a diffusion-controlled current flow due to electroreduction of the C$_{18}$MV^{2+} molecules which diffuse laterally along the oxide pores to the electrode surface. In the course of the experiment, an integral of the current (Q) is recorded as a function of time. Solution of the Fick's laws of diffusion with a set of boundary conditions appropriate for this case yields the following equation predicting a linear dependence of Q vs. $t^{1/2}$ (Bard and Faulkner, 1980b)

$$Q = 2Q_f D^{1/2} t^{1/2}/(d\pi^{1/2}) = S t^{1/2} \qquad (3)$$

where Q_f is the charge equivalent to the complete one-electron reduction of all C$_{18}$MV^{2+} present in the system, D is the lateral diffusion coefficient of C$_{18}$MV^{2+}, and d is the thickness of the porous aluminum oxide film (the length of the oxide channels supporting the OTS/C$_{18}$MV^{2+} bilayer assemblies).

Typical data (in terms of Q vs. $t^{1/2}$ plots) collected over 10-s time intervals in a series of experiments are shown in Fig. 5. The initial linear segments in curves A–C observed for $t < 0.6$ s correspond to the diffusion controlled process described by Eq. 3. The significant decrease of the slopes of these plots at longer times is due to the limited thickness of the oxide films (∼3.0 μm) and marks the end of the so-called semi-infinite regime in the system's behavior. This happens when the initial surface concentration of C$_{18}$MV^{2+} in the outermost part of the oxide film away from the electrode surface, begins to decrease as a result of the continuing electroreduction and the ensuing diffusion of C$_{18}$MV^{2+} toward the electrode. The second linear segment of the Q vs. $t^{1/2}$ plots is due to the background current (this probably includes current due to reduction of traces of oxygen that is difficult to purge completely from amphiphilic systems). Indeed,
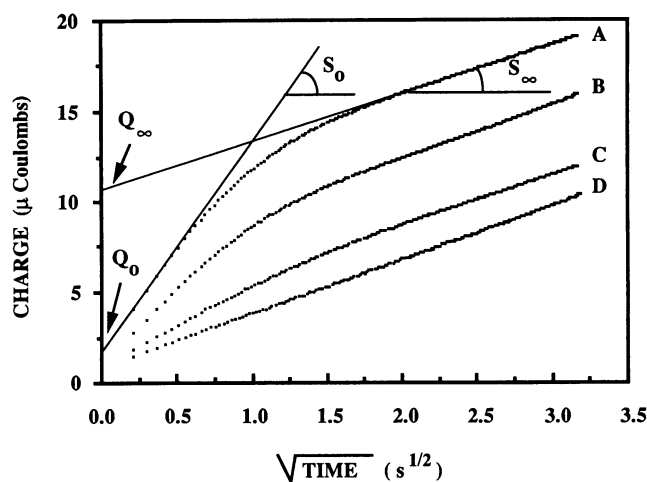
FIGURE 5   Typical chronocoulometric Q vs. $t^{1/2}$ plots recorded with $C_{18}MV^{2+}$/DMPC monolayers assembled on OTS-treated surfaces of porous aluminum oxide films carried out in 0.1 M pH 7.0 phosphate buffer. Initial potential, −0.25 V; final potential, 0.65 V vs. SCE. All self-assembly and electrochemical experiments were done at 30°C. DMPC coverage was greater or equal to 270 pmol/cm². Loading conditions: (A) 120-min exposure to 7.0 × 10⁻⁴ DMPC vesicle solution followed by a 30-min exposure to 5.0 × 10⁻⁴ M $C_{18}MV^{2+}$ solution and a medium transfer to a pure phosphate buffer electrolyte. $C_{18}MV^{2+}$ surface concentration 31 pmol/cm². (B) Same as A after 80 min incubation in a phosphate buffer. $C_{18}MV^{2+}$ surface concentration decreased to 18 pmol/cm². (C) Same as B after 30 min re-exposure to the DMPC loading solution. $C_{18}MV^{2+}$ surface coverage 7.4 pmol/cm². (D) Background run; same as A, except $C_{18}MV^{2+}$ loading.

curve D in Fig. 5, which was obtained in the absence of $C_{18}MV^{2+}$, has the same slope as those in *curves A–C* for $t > 2.5$ s.

To obtain Q_f, we subtracted Q_o, the intercept of Q vs. $t^{1/2}$ plots, from Q_∞ as marked in Fig. 5. The background intercept Q_o contains two components: the double-layer charge (required to change the electrode potential from the initial to its final value) and the charge due to the reduction of $C_{18}MV^{2+}$ that was adsorbed directly at the electrode surface in the self-assembly step. The value of the slope, S, in Eq. 3 is obtained by subtracting the background slope, S_∞, from the experimental slope, S_o, as shown in the figure. Thus, D is ultimately given by

$$D = \frac{1}{4} \pi d^2 \left[\frac{S_o - S_\infty}{Q_\infty - Q_o} \right]^2. \qquad (4)$$

As can be recognized from the above equation, the accuracy of the measurements of the lateral diffusion coefficients are strongly affected by the uncertainty in our measurements of the film thickness, d, that is known only to within ± 10%. This results in a ±20% error in D. In addition, errors involved in the measurements of the slopes and intercepts limit the precision of S and Q_∞ to within ± 10% for the lowest $C_{18}MV^{2+}$ coverages and to 1 or 2% for high coverages of the viologen amphiphile. Thus, the overall precision of the chronocoulometric measurements of D is between ±20% and ±40%.

The chronocoulometric method discussed above was used to investigate lateral mobility of $C_{18}MV^{2+}$ in single com-

ponent bilayers on OTS and in mixed assemblies with DMPC ($C_{18}MV^{2+}$+DMPC)/OTS. In the case of pure octadecylviologen monolayers, the results in Fig. 6 show that the $C_{18}MV^{2+}$ lateral diffusion coefficient (1.1×10^{-7} cm²/s) is largely independent of the $C_{18}MV^{2+}$ surface coverage. Although this behavior has been observed before for this amphiphile under slightly different conditions, it remains not fully understood (Miller et al., 1988). One explanation is that in the concentration range covered in these experiments (<40% full coverage), $C_{18}MV^{2+}$ aggregates to form microscopic domains or islands of higher but constant surface concentration. Progressively longer loading times increase the fraction of the OTS surfaces covered with $C_{18}MV^{2+}$ domains while their fluidity is constant. The other explanation of the invariance of D with $C_{18}MV^{2+}$ coverage in Fig. 6 postulates that $C_{18}MV^{2+}$ coverage is sufficiently low so that $C_{18}MV^{2+}$ monolayer is partially collapsed on the OTS surface and that diffusion of the individual $C_{18}MV^{2+}$ molecules is limited by their drag interactions with the OTS surface and thus remains constant. One example of such a scenario has been described previously (Goss and Majda, 1991), and thus we believe that this explanation of the $C_{18}MV^{2+}$ data in Fig. 6 is preferable.

Behavior of $C_{18}MV^{2+}$ in mixed monolayers with DMPC as illustrated in Fig. 6 is substantially different. In these experiments, we followed the procedure of Fig. 4 in the formation of the mixed assemblies that exposed OTS-treated oxide films first to a DPPC vesicle solution for a variable period of time, followed by the loading of $C_{18}MV^{2+}$. In view of the data in Fig. 4, it is apparent that at low $C_{18}MV^{2+}$ coverages, its diffusion coefficient approximates that which prevails in a DMPC monolayer. As the $C_{18}MV^{2+}$ surface concentration increases, due to a lower surface concentration of DMPC, D increases due to a higher intrinsic fluidity of pure $C_{18}MV^{2+}$ monolayers. The latter is likely related to a charge repulsion in the head-group
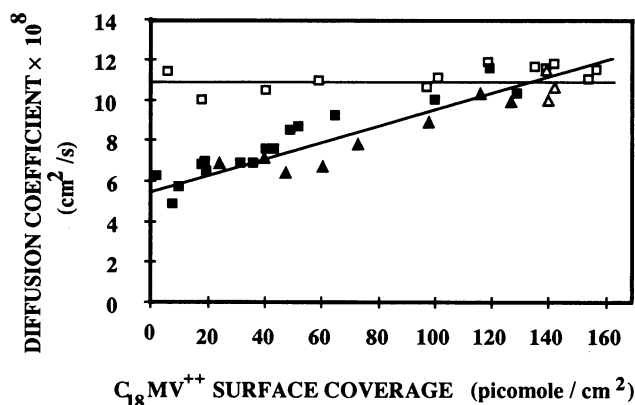

FIGURE 6   Dependence of the $C_{18}MV^{2+}$ lateral diffusion coefficient on the $C_{18}MV^{2+}$ surface concentration in self-assembled monolayers on OTS-treated surfaces of porous aluminum oxide films. *Open symbols:* pure $C_{18}MV^{2+}$ monolayers. *Closed symbols:* mixed monolayers were formed by exposure to DMPC (*squares*) or DPPC (*triangles*) solutions followed by $C_{18}MV^{2+}$ loading as in Fig. 3.

region and lower density of the hydrocarbon chains in the octadecylviologen monolayers.

To obtain a meaningful measurement of the translational diffusion coefficient in a lipid monolayer, we needed to carry out our experiments with lipid monolayers at concentrations closely resembling those characteristic for lipid bilayers (Fig.4) and with as low concentrations of an electroactive probe as possible. To meet these criteria and yet to cover at least a small range of $C_{18}MV^{2+}$ concentrations, we carried out two series of experiments. In the first series, designed to address a higher end of $C_{18}MV^{2+}$ concentrations, we followed the protocol of Fig. 3 with one important modification. Namely, the radioactive assay technique was used to determine the surface concentration of a lipid after the incubation of a substrate in $C_{18}MV^{2+}$ loading solutions. These measurements showed that approximately 15% of a lipid is desorbed during a 30-min exposure to the $C_{18}MV^{2+}$ loading solution. The latter was determined by the voltammetric method of Fig. 2, and the chronocoulometry was then used to obtain its lateral diffusion coefficient. In these experiments, DMPC surface concentration ranged from 200 to 240 pmol/cm², while $C_{18}MV^{2+}$ concentration varied from 65 to 30 pmol/cm², respectively. All experiments were done at 30°C. The variation of D with the mole fraction of $C_{18}MV^{2+}$ is shown in Fig. 7 (squares).

In the second series of experiments, incubation of the oxide-coated electrodes in the DMPC vesicle solution was carried out for 120 min at 30°C to obtain the maximum equilibrium coverage. Subsequently the electrodes were transferred to the $C_{18}MV^{2+}$ loading solution for 30 min, resulting in the incorporation of 30–40 pmol/cm² $C_{18}MV^{2+}$. The radioactive assay gave the final DMPC coverage of ~220 pm/cm². The same electrodes were then again incubated for an increasing period of time (50–140 min) in the DMPC vesicle solution at 4°C to gradually decrease the $C_{18}MV^{2+}$ surface concentration. Independent measurements showed that this

procedure restores the DMPC surface concentration to the maximum level of ~300 pmol/cm². This is the same level as the limiting value obtained at 18°C in Fig. 4. This progressive $C_{18}MV^{2+}$ leaching experiment was interrupted several times to transfer an electrode to the usual 0.1 M phosphate buffer at 30°C and to measure $C_{18}MV^{2+}$ coverage and D. The lateral diffusion coefficients versus $C_{18}MV^{2+}$ molar fraction in DMPC monolayer resulting from these experiments are plotted in Fig. 7 (circles).

Data in Fig. 7 cover a range of $C_{18}MV^{2+}$ mole fractions from 25 to 0.7 mol %. The linearity of the plot provides a strong indication that $C_{18}MV^{2+}$ is fully miscible with DMPC. The limiting value of D extrapolated to zero $C_{18}MV^{2+}$ coverage, 5 × 10⁻⁸ cm²/s, reflects the fluidity of the DMPC monolayer. Since the size of $C_{18}MV^{2+}$ molecule is not substantially different from DMPC, the limiting value of $C_{18}MV^{2+}$ diffusion coefficient in Fig. 7 is a good approximation of DMPC lateral diffusion coefficient. Indeed, very similar values of D_{DMPC} measured by FRAP method were reported recently in the literature. For example, 3.0 × 10⁻⁸ cm² s⁻¹ (at 24°C) was obtained for supported monolayers on alkylated glass surfaces by Tscharner and McConnell (1981); 4.0 × 10⁻⁸ cm² s⁻¹ (at 30°C) was reported for supported bilayers on glass (Tamm and McConnell, 1985); 6.0 × 10⁻⁸ cm² s⁻¹ and 5.0 × 10⁻⁸ cm² s⁻¹ (at 30°C) were obtained for multibilayers by Vaz and co-workers (1985) and by Chazotte and co-workers (1991), respectively.

We next examine the temperature dependence of $D_{C_{18}MV^{2+}}$ in lipid monolayers. The chronocoulometric experiments were carried out with ~6 mol % of $C_{18}MV^{2+}$ in lipid monolayers ($C_{18}MV^{2+}$ concentration ranged from 3 to 8 mol %) in the temperature range from 18 to 45°C. The lipid monolayers were formed by the usual adsorption and fusion of lipid vesicles for 120 min at 40°C, followed by $C_{18}MV^{2+}$ loading at 30°C. Electrochemical measurements at a particular temperature were done both during a heating up and a cooling down cycle to examine the possibility of histeretic behavior. None was observed. The Arrhenius plots are shown in Fig. 8. Both pure $C_{18}MV^{2+}$ monolayers and lipid monolayers gave linear plots. No evidence of phase transitions in either case (including DPPC monolayers; data not shown) was found in spite of the fact that the differential scanning calorimetry measurements of the DPPC and DMPC vesicle solutions showed, as expected, the chain-melting phase transition temperatures at 42 and 23°C, respectively. The activation energy for DMPC system of 39 kJ/mol is in reasonable agreement with 43.7 kJ/mol obtained by Tamm and McConnell for the DMPC bilayers on silicon dioxide (formed by Langmuir-Blodgett transfer at 36.5 dyn/cm) above 28°C (Tamm and McConnell, 1985). The similarity of the activation energy values for DMPC and pure $C_{18}MV^{2+}$ monolayers in Fig. 8 is clearly coincidental.

These results lead us to the following main conclusions. First, the supported lipid bilayers examined in these studies appear to be homogeneous and do not exhibit phase transitions that are usually observed for these systems in vesicles (McConnell et al., 1984), monolayers on the water surface
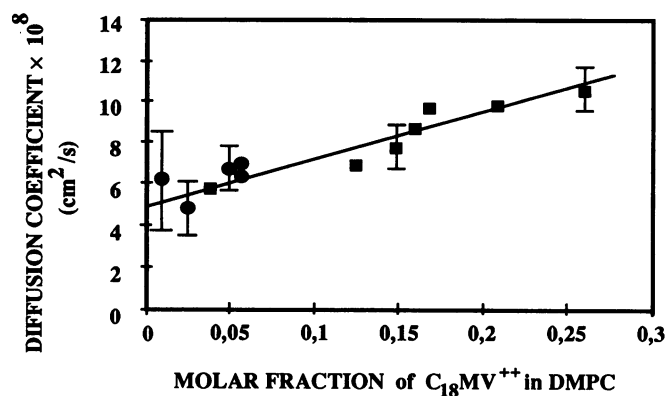

FIGURE 7   Dependence of the $C_{18}MV^{2+}$ lateral diffusion coefficient on the $C_{18}MV^{2+}$ surface concentration in DMPC monolayers on OTS-treated Al_2O_3 surfaces. Data marked with squares were obtained with DMPC surface concentration increasing from 200 to 240 pmol/cm² as the mole fraction of $C_{18}MV^{2+}$ decreased from 27% to 4%. Data marked with circles were obtained with DMPC coverage of ~220 pmol/cm². (See text for more procedural details.)
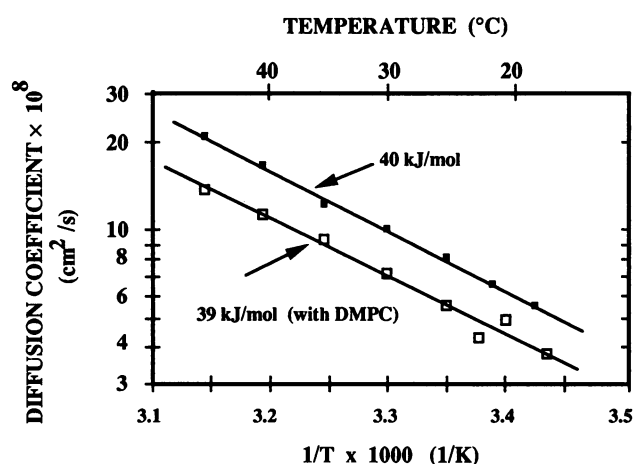
FIGURE 8   Arrhenius plots of $C_{18}MV^{2+}$ lateral diffusion coefficient in pure $C_{18}MV^{2+}$ monolayers and $DMPC/C_{18}MV^{2+}$ monolayers on OTS-treated surfaces of porous aluminum oxide films. Surface concentration of $C_{18}MV^{2+}$ in mixed monolayers was ~6 mol %. Data points represent averages of two to four measurements done during heating and cooling parts of the temperature cycles.

(Peters and Beck, 1983) or in Langmuir-Blodgett bilayers (Tamm and McConnell, 1985; McConnell et al., 1986). Moreover, the fluidity of the lipid monolayers assessed at 30°C appears to be independent of the temperature at which they were formed (above or below the main chain-melting phase transition) despite some differences in the maximum lipid surface concentrations observed with temperature (Fig. 4). This suggests that the lipid-OTS interactions in the mid-plain of the bilayer are responsible for the lack of phase transitions and for maintaining the monolayers in their fluid state. Similar behavior was observed by Tscharner and McConnell, who reported an essentially constant diffusion coefficient of $\sim 10^{-8}$ cm^2/s in supported DPPC monolayers on OTS-treated glass slides unless the lipid monolayer was transferred from the water surface in the solid-condensed state (Tscharner and McConnell, 1981). In other words, the supported DPPC monolayers did not retain their phase behavior (LE, LE/LC, LC, and S) and became homogeneous after transfer onto the alkylated surface even if the experiments were carried out below T_m. Consistency of our results with these and related literature data (Naumann et al., 1992) suggests that the observed inability to form lipid monolayers in solid condensed state by vesicle fusion (Figs. 7 and 8) is indeed the property of the system and not an artifact introduced by the electroactive probe species. We may thus reach a general conclusion that the chronocoulometric method of measuring lateral diffusion coefficients described in this report can be applied successfully to lipid monolayer assemblies.

Lateral diffusion of ubiquinone in supported lipid bilayers

Application of the chronocoulometric method described above to the studies of electrochemically active species is particularly advantageous since their diffusion could be investigated without the deleterious side effects usually associated with attachment of a fluorescence or other label moieties to species of interest. Ubiquinone (Q_{50}) is one such example. Several attempts to investigate its lateral mobility in lipid bilayers were made, all involving FRAP method and thus burdened with the uncertainties mentioned above (Chazotte et al., 1991; Rajarathnam et al., 1989; Gupte et al., 1984). Consequently, the rate of ubiquinone diffusion, its location in lipid bilayers, and a number of related issues remain unknown or at best controversial. In this section, we present our preliminary results reporting a diffusion coefficient of ubiquinone in OTS/DMPC bilayer assemblies obtained by the chronocoulometric method.

The experimental procedures were, in general, analogous to those described above. OTS-treated porous aluminum oxide films on gold electrodes were exposed for 60 min at 30°C to the DMPC vesicle solutions containing 5 mol % ubiquinone. Subsequently, electrode substrates were rinsed and transferred to 0.1 M phosphate buffer solution in an electrochemical cell. A typical cyclic voltammogram of ubiquinone obtained in such an experiment is shown in Fig. 9. Electroactivity of ubiquinone, which under present conditions is expected to be confined predominantly to the hydrocarbon region of the supported bilayers, appears to be consistent with a $2H^+$, $2e^-$ reduction and oxidation reported previously for this pH (Takehara et al., 1991; Schrebler et al., 1990; Ksenzhek et al., 1982). This rough mechanistic assignment requires more thorough studies to be verified. Nevertheless, with this uncertainty in mind, we may calculate the apparent surface concentration of Q_{50} in the supported bilayer by integrating the cathodic peak current above background. This gave us surface coverage of ~8.6 pmol/cm^2 (in a number of experiments with different electrodes, this ranged from 5 to 10 pmol/cm^2), which corresponds to 3.0 mol % of the lipid monolayer (1.7 to 3.3 mol % for the whole series of electrodes), a value consistent with ubiquinone content in mitochondrial membranes.
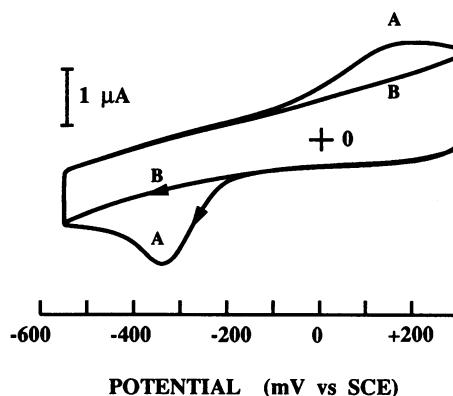

FIGURE 9   Cyclic voltammetry of ubiquinone in DMPC/OTS bilayer assemblies in porous aluminum oxide films recorded in 0.1 M pH 7.0 phosphate buffer at 50 mV/s. Ubiquinone surface concentration 8.6 pmol/cm^2 or 3.0 mol % of the DMPC coverage; $T = 30$°C.

The value of the diffusion coefficient for Q_{50} obtained by chronocoulometry using the experimental protocol and data analysis of Fig. 5 was $1.9 \pm 0.4 \times 10^{-8}$ cm^2/s at 30°C obtained on the basis of 15 measurements with three different electrodes. The experiments involved application of a negative potential pulse from -0.100 V to -0.500 V vs. SCE. This value of D is approximately 2 to 3 times smaller than the diffusion coefficient of DMPC under otherwise identical conditions. This is consistent with the larger size of Q_{50} compared to lipid molecules. This preliminary value of the Q_{50} diffusion coefficient is similar to those reported in the literature for fluorescently labeled ubiquinone and its shorter chain derivatives (Chazotte et al., 1991; Rajarathnam et al., 1989; Gupte et al., 1984). More detailed investigations of this system using our electrochemical methods are currently in progress in our laboratories.

CONCLUSIONS

This report demonstrates the usefulness of electrochemical techniques to investigate lateral processes in lipid monolayer assemblies. These are the first electrochemical measurements of the lateral diffusion coefficients in supported phospholipid monolayers. Specifically, we have shown the application of cyclic voltammetry and chronocoulometry in determining lateral fluidity of DMPC, DPPC, and lateral diffusion constant of ubiquinone in supported lipid bilayers. The fluidity of the supported DMPC and DPPC monolayers was deduced from the measurements of the lateral diffusion coefficient of an electroactive amphiphile, $C_{18}MV^{2+}$. The latter was incorporated into lipid monolayers at variable mole fractions (0.7–20 mol %). We have shown that the limiting value of the octadecylviologen diffusion coefficient, 5×10^{-8} cm^2/s at 30°C, as its mole fraction approaches 0, approximates very well the lateral diffusion coefficient of the phospholipids. These results and the temperature studies, in which linear Arrhenius plots were observed between 18 and 45°C with activation energies of $\sim$40 kJ/mol, demonstrate that lipid monolayers remain homogeneous and do not undergo the phase transitions known for these systems from the monolayer studies at the air/water interface.

Sonication of DMPC in presence of 5 mol % of ubiquinone results in the formation of vesicles incorporating both of these components. Their adsorption and fusion onto OTS treated aluminum oxide templates leads to the formation of supported monolayers that contain, according to the voltammetric assay, 3 mol % of ubiquinone, a concentration consistent with the physiological conditions in mitochondrial membranes. Chronocoulometric measurements were used to determine a preliminary value of ubiquinone lateral diffusion coefficient to be approximately $1.9 \pm 0.4 \times 10^{-8}$ cm^2/s at 30°C. Intrinsic electroactivity of ubiquinone allowed us to determined this value without any structural modification of ubiquinone that are otherwise necessary when FRAP method is used as a traditional measurement tool in the studies of the membrane lateral processes. Methodology described in this report opens new possibilities in the investigations of naturally occurring redox carriers in biological membrane systems.

REFERENCES

Bard, A. J., and L. R. Faulkner. 1980a. Electrochemical Methods: Fundamentals and Applications. John Wiley and Sons, New York. 130–134.

Bard, A. J., and L. R. Faulkner. 1980b. Electrochemical Methods: Fundamentals and Applications. John Wiley and Sons, New York. 199–206.

Bard, A. J., and L. R. Faulkner. 1980c. Electrochemical Methods: Fundamentals and Applications. John Wiley and Sons, New York. 406–413.

Brian, A. A., and H. M. McConnell. 1984. Allogeneic stimulation of cytotoxic T cells by supported planar membranes. Proc. Natl. Acad. Sci. USA. 81:6159–6163.

Charych, D. H., E. M. Landau, and M. Majda. 1991. Electrochemistry at the air/water interface. Lateral diffusion of an octadecylferrocene amphiphile in Langmuir monolayers. J. Am. Chem. Soc. 113:3340–3346.

Chazotte, B., E. S. Wu, and C. R. Hackenbrock. 1991. The mobility of a fluorescent ubiquinone in model lipid membranes. Relevance to mitochondrial electron transport. Biochim. Biophys. Acta. 1058:400–409.

Cherry, R. J. 1979. Rotational and lateral diffusion of membrane proteins. Biochim. Biophys. Acta. 559:289–327.

Gennis, R. B. 1989. Biomembranes, molecular structure and function. Springer-Verlag, New York. 533 pp.

Goss, C. A., and M. Majda. 1991. Lateral diffusion in organized bilayer assemblies of electroactive amphiphiles. Influence of the oxidation state of the amphiphile investigated by steady-state methods involving an interdigitated micro-electrode array device. J. Electroanal. Chem. 300: 377–405.

Goss, C. A., C. J. Miller, and M. Majda. 1988. Microporous aluminum oxide films at electrodes. 5. Mechanism of the lateral charge transport in bilayer assemblies of electroactive amphiphiles. J. Phys. Chem. 93:1937–1942.

Gupte, S., E. S. Wu, L. Hoechli, M. Hoechli, K. Jacobson, A. E. Sowers, and C. R. Hackenbrock. 1984. Relationship between lateral diffusion and collision frequency, and electron transfer of mitochondrial inner membrane oxidation-reduction components. Proc. Natl. Acad. Sci. USA. 81: 2606–2610.

Hackenbrock, C. R. 1981. Lateral diffusion and electron transfer in the mitochondrial inner membrane. Trends Biochem. 6:151–154.

Kalb, E., S. Frey, and L. K. Tamm. 1992. Formation of supported planar bilayers by fusion of vesicles to supported phospholipid monolayers. Biochim. Biophys. Acta. 1103:307–316.

Kim, S., and H. Yu. 1992. Lateral diffusion of amphiphiles and macromolecules at the air-water interface. J. Phys. Chem. 96:4034–4040.

Krieg, M., M. P. Pileni, A. Braun, and M. Gratzel. 1981. Micelle formation and surface activity of functional redox relays: viologens substituted by a long alkyl chain. J. Colloid Interface Sci. 83:202–213.

Ksenzhek, O. S., S. A. Petrova, and M. V. Kolodyazhny. 1982. Redox properties of ubiquinones in aqueous solutions. Bioelectrochem. Bioenerg. 9:167–174.

Lindholm-Sethson, B., J. T. Orr, and M. Majda. 1993. Lateral diffusion of an octadecylferrocene amphiphile in Langmuir-Blodgett bilayer assemblies. Effects of the amphiphile concentration. Langmuir 9:2161–2167.

Majda, M. 1991. Dynamics of lateral charge transport in bilayer assemblies of electrochemically active amphiphiles. In Kinetics and Catalysis in Microheterogeneous Systems (Surface Science Series). Vol. 38. M. Grätzel and K. Kalyanasundaram, editors. Marcel Dekker, New York. 227–272.

Majda, M. 1994. Translational diffusion and electron hopping in monolayers at the air/water interface. In Organic Thin Films and Surfaces. Vol. 1. A. Ulman, editor. Academic Press, New York. In press.

Maoz, R., and J. Sagiv. 1983. On the formation and structure of self-assembling monolayers. A comparative ATR wettability study of Langmuir-Blodgett and adsorbed films on flat substrates and glass microbeads. J. Colloid Interface Sci. 100:465–496.

McConnell, H. M., L. K. Tamm, and R. M. Weis. 1984. Periodic structures in lipid monolayer phase transitions. *Proc. Natl. Acad. Sci. USA.* 81: 3249–3253.

McConnell, H. M., T. H. Watts, R. M. Weis, and A. A. Brian. 1986. Supported planar membranes in studies of cell-cell recognition in the immune system. *Biochim. Biophys. Acta.* 864:95–106.

Miller, C. J., and M. Majda. 1986. Microporous aluminum oxide films at electrodes. 2. Studies of electron transport in the Al_2O_3 matrix derivatized by absorption of poly(4-vinylpyridine). *J. Electroanal. Chem.* 207:49–72.

Miller, C. J., C. A. Widrig, D. H. Charych, and M. Majda. 1988. Microporous aluminum oxide films at electrodes. 4. Lateral charge transport in self-organized bilayer assemblies. *J. Phys. Chem.* 92:1928–1936.

Naumann, C., T. Brumm, and T. M. Bayerl. 1992. Phase transition behavior of single phosphatidylcholine bilayers on a solid spherical support studied by DSC, NMR, FT-IR. *Biophys. J.* 63:1314–1319.

Parpaleix, T., J. M. Laval, M. Majda, and C. Bourdillon. 1992. Potentiometric and voltammetric investigations of H_2/H^+ catalysis by periplasmic hydrogenase from *Desulfovibrio gigas* immobilized at the electrode surface in an amphiphilic bilayer assembly. *Anal. Chem.* 64: 641–646.

Peters, R., and K. Beck. 1983. Translational diffusion in phospholipid monolayers measured by fluorescence microphotolysis. *Proc. Natl. Acad. Sci. USA.* 80:7183–7187.

Pileni, M. P., A. M. Braun, and M. Grätzel. 1980. Light driven redox processes in functional micellar units. III, Zn-tetraphenylporphyrin sensitized reactions in methyl viologen surfactant assemblies. *Photochem. Photobiol.* 31:423–427.

Rajarathnam, K., J. Hochman, M. Schindler, and S. Ferguson-Miller. 1989. Synthesis, location, and lateral mobility of fluorescently labeled ubiquinone 10 in mitochondrial and artificial membranes. *Biochemistry.* 28: 3168–3176.

Schrebler, R. S., A. Arratia, S. Sanchez, M. Haun, and N. Duran. 1990. Electron transport in biological processes. Electrochemical behavior of ubiquinone absorbed on a pyrolytic graphite electrode. *Bioelectrochem. Bioenergetics* 23:81–91.

Singh, S., and D. J. Keller. 1991. Atomic force microscopy of supported planar membrane bilayers. *Biophys. J.* 60:1401–1410.

Takehara, K., H. Takemura, Y. Ide, and S. Okayama. 1991. Electrochemical behavior of ubiquinone and vitamin K incorporated into n-alkanethiol molecular assemblies on a gold electrode. *J. Electroanal. Chem.* 308: 345–350.

Tamada, K., S. Kim, and H. Yu. 1993. Lateral diffusion of a probe lipid in biphasic phospholipid monolayers: liquid/gas coexistence films. *Langmuir* 9:1545–1550.

Tamm, L. K., and H. M. McConnell. 1985. Supported phospholipid bilayers. *Biophys. J.* 47:105–113.

Tscharner, V. V., and H. M. McConnell. 1981. Physical properties of lipid monolayers on alkylated planar glass surfaces. *Biophys. J.* 36:421–427.

Vaz, W. L. C., and P. F. Almeda. 1991. Microscopic versus macroscopic diffusion in one-component fluid phase lipid bilayer membranes. *Biophys. J.* 60:1553–1554.

Vaz, W. L. C., R. M. Clegg, and D. Hallmann. 1985. Translational diffusion of lipids in liquid crystalline phase phosphatidylcholine multibilayers. A comparison of experiment with theory. *Biochemistry.* 24:781–786.